AMERICAN JOURNAL OF MATERIALS AND NANOTECHNOLOGY

A Numerical Wear Simulation Method of Reciprocating Seals with a Textured Rod

Hongliang Ran [1,2], Di Liu [1] and Shaoping Wang [1,3,4,*]

1 School of Automation Science and Electrical Engineering, Beihang University, Beijing 100083, China;
2 Equipment Support Department, Logistics University of PAP, Tianjin 300309, China
3 Beijing Advanced Innovation Center for Big Data-based Precision Medicine, Beihang University, Beijing 100191, China
4 Ningbo Institute of Technology, Beihang University, Ningbo 315800, China *

Abstract: Reciprocating rod seals are widely used in the hydraulic actuator to prevent the leakage of fluid. The sealing lip profile changes with the seal wear, resulting in an increase in the leakage. A texturing rod changes the lubrication characteristics of the seal, so it a ects the wear and leakage of the seal. A numerical simulation method is proposed to investigate the wear of the hydraulic reciprocating seal with textured rods. Several kinds of macro-cavity textures on the rod surface, including circle, square and triangle shapes, have been simulated and discussed. The e ects of three shape parameters including area ratio, depth, and ratio of the axial length to the circumferential length on the seal wear are analyzed in detail. The texturing rod slightly increases the seal wear, but decreases the seal leakage. When the rod speed is increasing, the wear time rates of the seal increase, while the wear distance rates decrease, regardless of the texture shapes. When the texture area ratio is increasing, the wear of the reciprocating seal increases. Seal wear decreases with an increasing texture depth during the outstroke, however, it increases during the instroke. The ratio of the axial length of the macro-cavity to the circumferential length has no e ect on the seal wear.

Keywords: reciprocating seal; texturing rod; seal wear; lubrication characteristics; leakage

1. Introduction

Elastic seals are critical components and widely used in hydraulic systems to prevent the leakage of the fluid [1,2]. As one of the dynamic elastic seals, reciprocating rod seals are widely used in hydraulic actuators [3,4]. If the seal fails, the leakage of actuator would not only pollute the environment, but also cause the loss of working capacity. Thus, the hydraulic system is significantly a ected by the performance of the reciprocating seal.

Many published research about the reciprocating seals, such as the O-ring [5], VL seal [6,7], and so on [8,9], have clarified the relationships between the performance with the operating conditions. With improvements in the laser surface processing technology, laser texturing surface for improving the performances of mechanical components has attracted extensive attention [10–12]. Especially, improving seal performances by a texturing rod is an important topic for the seals. Huang et al. [13] analyzed the performances of the reciprocating seal with plunge ground rods. The contact pressure, friction force and fluid transport are simulated and discussed by a mixed lubricating model. The seal performances of the reciprocating seal with textured rod have also been numerically studied in Ref. [14]. Gadari et al. [15] numerically analyzed the sealing mechanism of reciprocating seal with grooved rod. The lubrication film and fluid pressure distributions are simulated by the modified Reynolds equation considering the cavitation on the sealing zone. A comparison between experimental and numerical results has shown that the method is more accurate than the inverse hydrodynamic lubrication (IHL) model. In addition, Guo et al. [16,17] investigated the e ects of the textured shafts on the performances of rotary lip seal. It is found that the textured shafts would change the pumping rate and friction torque of the shaft lip seal.

Since the seal is operating under mixed lubricating conditions, the wear of the reciprocating seal is unavoidable due to friction and wear, the sealing lip is thus continuously changed when the seal is working [18]. With the change of the lip profile, the contact width and contact pressure on the sealing zone are changed accordingly. Since the sealing performance is significantly dependent on the contact width and contact pressure, the wear of the sealing lip would lead to a continuous change of the sealing behaviors, including friction, leakage, and so on [19].

Some previous research on the seal wear mainly concentrate on the experimental aspects. Combing the experiment with the numerical model, the influence of the wear of the seal lip on the performance of the shaft lip seal was studied [18]. The wear properties of the seal materials were investigated by experiments, including accelerated wear [20], and two-body abrasive wear [21], and so on [22,23]. However, since there are many parameters to be considered and controlled in the experiments, the experimental studies are normally time consuming and expensive. Numerical approaches have thus been used to study on the wear of the seal. Due to the widely used of Finite element method (FEM) in the structural analysis [24], a combination of the FEM and Archard wear model is normally adopted to simulate the seal wear [25]. The contact pressure is calculated by finite element analysis (FEA). The wear depth of the seal lip is solved by the Archard wear model. Békési et al. [26,27] simulated the wear process of the reciprocating seal. Considering the e ects of temperature, a structural and thermal coupling simulation model is developed based on the FEM to study the wear of the seals, including the O-shape seal and rectangular-section seal [28,29]. The continuous wear process is approximated as a discrete set of time. The wear depth is calculated by the Archard wear model and used to update the seal lip geometry. Frölich et al. [23] presented a macroscopic simulation model for analyzing the contact behavior of a rotary lip seal, considering the interaction of temperature, friction and wear.

However, the method of combing the FEM and Archard wear model neglects the lubricating e ects on the wear of the seal. In fact, lubrication characters and wear of the seal are strongly coupled. To this end, the e ects of the lubrication on the seal wear should not be neglected when analyzing the seal wear. To investigate seal wear under di erent lubricating conditions, a numerical wear model is proposed in Ref. [30] based on the elasto-hydrodynamic (EHD) lubrication model, Archard wear model and macro contact model. The relationship between the lubricating characteristics and the seal wear was analyzed. In addition, a multiscale simulation model was made to analyze the relationship between seal wear and lubrication characteristics in Refs. [31,32]. In the simulations, macro contact load is analyzed by the macroscale finite element model. Asperity contact and hydrodynamic pressures are calculated by a mixed thermal EHD lubrication model. The Archard model is modified to calculate the seal wear.

For the textured surface, Xiong et al. [33] studied the sliding wear of polytetrafluoroethylene (PTFE) experimentally. Qi et al. [34] investigated the e ects of the textured steel surface on the tribological properties of PTFE composite in dry friction. Moreover, the e ects of the textured shafts on the wear of the rotary lips seal were analyzed in Ref. [35]. However, it is di cult to find a study on the e ects of the textured rod on the wear of the reciprocating seal. In addition, since the experimental studies are always time consuming and labor consuming, a numerical wear simulation method is presented in this paper for reciprocating seals with textured rods. Three common kinds of texture shapes, such as circle, square, and triangle, are modeled and investigated. The e ects of the lubricating characteristic of the reciprocating seal are considered in the numerical model. Under di erent rod speeds and di erent texture parameters, the wear of the reciprocating seal is simulated and discussed.

The structure of the rest of the paper is as follows. Rod textures and shape feature parameters are introduced in Section 2. In Section 3, the lubrication model is developed with considering the rod

zone. Generally, the lubricating film on the sealing zone is only a few microns. So, the microscopic deformation of the sealing lip caused by the lubricating film is very small. Compared with the macro deformation, the micro deformation on the sealing lip so small that it is assume the micro deformation has no e ects on the macroscopic deformation of the seal. Namely, the static contact pressure and contact width will not change with the microscopic deformation of the sealing lip.

The simulation of the microscopic deformation is divided into two parts. Firstly, the calculation of the microscopic deformation on seal surface with a smooth rod is produced. Since the reciprocating seal is under the mixed operating conditions, asperity contact occurs and the ratio of the film thickness to the surface roughness is less than three. Therefore, the micro deformation of the seal lip caused by the film is very little. Compared with the micro deformation of the seal lip, the total size of the seal is so large that the seal can be considered as a semi-infinite body [4]. Therefore, the calculation of the seal microscopic deformation is given by

$$Dh(x, y) = \underset{\text{Simulation space}}{x} \left(\frac{1 \ \ seal^2}{E_{seal}} \frac{Dp(\ , \#)}{q \ \ \ \ \ 2 \ \ \ \ \ 2} \right) d \ d\# \quad (14)$$

$$(15)$$

The local pressure di erence $Dp(x, y)$ is given by

$$Dp(x, y) = p_f(x, y) + p_c(x, y) \ \ p(x, y)$$

where p is the static contact pressure.

Secondly, the microscopic deformation of the seal caused by the textures on the rod is simulated. After the calculation in the first simulation, the pressure di erence in the non-textured zone is zero, the sum of the pressure di erences in the textured zone is

$$F_{sum} = \underset{\text{textured zone}}{x} (p_f(x, y) + p_c(x, y)) \ \ p(x, y)dxdy \quad (16)$$

Since the seal is viscoelastic, when the rod moving there is not enough time for the seal surface to fall into the micro-cavity of the textured rod. Hence, the pressure di erence in the textured zone is undertaken by the non-textured zone [14]. During the movement of the rod, the texture on the sealing zone is changed all the time. It is assumed that the force di erence on the sealing zone is spread equally across the simulation area, the deformation of the seal lip surface is then calculated by Equation (14) with the following pressure di erence

$$Dp(x, y) = \frac{F_{sum}}{L_x L_y} \quad (17)$$

4. Wear Analysis

The Archard model is commonly applied to calculate the seal wear [23–30]. In the Archard wear model, the wear volume is calculated by

$$V = \frac{K}{H} WS \quad (18)$$

where V is the material wear volume, K is the wear coe cient, S is the relative sliding distance of surface, W is the normal load on the surface, H is the hardness of softer material.

where p_n is the normal contact pressure.

Generally, the wear modulus is obtained experimentally under a specific condition, in the wear analysis, it is assumed to be constant. However, as shown in Figure 5, the reciprocating rod seal is normally operated in mixed lubrication conditions. With the change of the operating conditions,

the lubrication characteristics of the seal on the sealing zone are changed accordingly. Especially, when the rod is textured, the lubrication characteristics change significantly. Therefore, the previous method is not suitable for analyzing the reciprocating seal with the textured rod, the Archard model should be modified for considering the lubrication.

lubrication characteristics of the seal on the sealing zone are changed accordingly. Especially, when the rod is textured, the lubrication characteristics change significantly. Therefore, the previous rod, the Archard model should be modified for considering the lubrication.

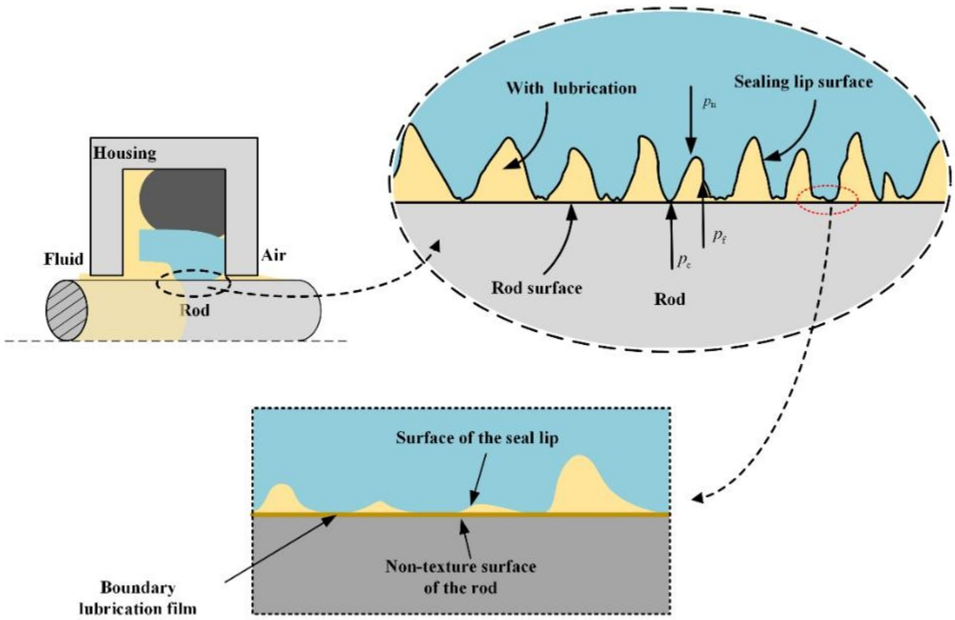

Figure 5. Detailed lubrication statuss on the sealing zone.

In the mixed lubrication conditions, the normal load of the sealing lip is composed of the fluid and asperity contact pressures, namely,

In the mixed lubrication conditions, the normal load of the sealing lip is composed of the fluid and asperity contact pressures, namely,

$$p_n = p_f + p_c \tag{22}$$

$$p_n = p_f + p_c \tag{22}$$

When the fluid is so clean that there is no particle in the lubricating film, the seal wear caused by the fluid pressure can be considered to be zero [35]. In this case, only asperity contact would cause seal wear. The wear depth of the reciprocating rod seal is calculated by

When the fluid is so clean that there is no particle in the lubricating film, the seal wear caused by the fluid pressure can be considered to be zero [35]. In this case, only asperity contact would cause wear. The wear depth of the reciprocating rod seal is calculated by

$$h_W = k p_c S \tag{23}$$

$$h_W = k p_c S \tag{23}$$

where p_c is predicted by the lubrication analysis.

The contact of the seal with the rod surface at the asperity point is not direct and dry. Since there is lubrication fluid existing in the sealing region, there is a boundary lubrication film at the contact point, as shown in Figure 5. Therefore, the wear modulus k of the sealing lip should be obtained by the boundary lubrication experiment of the PTFE-based material sliding on a smooth face. According to the Ref. [41,42], the value of the wear modulus of the PTFE-based material is approximately 10^{-4}–10^{-6} mm^3/Nm. In the presented research, the wear modulus of the PTFE-based ring is assumed to be 1.2×10^{-5} mm^3/Nm.

The contact of the seal with the rod surface at the asperity point is not direct and dry. Since there is lubrication fluid the sealing region, there is boundary film at the contact point, as shown in Figure 5. Therefore, the wear modulus k of the sealing lip should be obtained by the boundary lubrication experiment of the PTFE-based material sliding on a smooth face. According to the Ref. [41,42], the value of the wear modulus of the PTFE-based material is approximately 10^{-4}–10^{-6} mm^3/Nm. ring is assumed to be 1.2 × 10^{-5} mm^3/Nm.

When the rod is moving, the lubricating characteristic of the sealing zone changes with time because the rod surface is textured. The asperity contact pressure of the seal changes all the time with the rod moving. So, the average asperity contact pressure of a certain stroke is adopted to calculate the seal wear. Here, the stroke can be assumed to be equal to the texture length L, and the continuous motion of the piston rod is divided into n states. The wear depth of the seal is given by

When the rod is moving, the lubricating characteristic of the sealing zone changes with time because the rod surface is textured. The asperity contact pressure of the seal changes all the time with the rod moving. So, the average asperity contact pressure of a certain stroke is adopted to calculate the seal wear. Here, the stroke can be assumed to be equal to the texture length L, and the continuous motion of the piston rod is divided into n states. The wear depth of the seal is given by

$$h_W = k\bar{p}_c L \tag{24}$$

where

$$\bar{p}_c = \frac{1}{n}\sum_{i=1}^{n}(p_c)_i \tag{25}$$

The wear volume is given by

$$V = \int^{D_{rod}}\int_{L_y} h_W \, dxdy \tag{26}$$

In the presented research, the wear time rate is given by

$$r_t = \frac{dV}{dt} \tag{27}$$

The wear distance rate is given by

$$r_s = \frac{dV}{dL} \tag{28}$$

5. Procedure of the Simulation Method

The computational procedure is presented in Figure 6. The mixed lubricating model is firstly solved, then the wear model is solved based on the lubrication analysis. In the lubrication analysis, the fluid mechanics, asperity contact mechanics, and the micro deformation of the sealing lip are strongly coupled. In order to solve this coupling problem, an iterative method is adopted in the numerical analysis.

At the beginning of the numerical analysis, static contact pressure and contact width are obtained by FEA with the software ANSYS. Initial film thickness h_0 is obtained by inversing Equation (9). In the solving of Equation (9), asperity contact pressure is assumed to be equal to the static contact pressure. There are three loops in the analysis of the lubrication of the reciprocating seal. The innermost loop is used to solve the fluid pressure of the film, including the Reynolds equation and Roelands equation. When solving the Reynolds equation, a finite volume method is applied to discretize Equation (4), and the tri-diagonal matrix algorithm (TDMA) method is applied to solve the finite volume discrete equations. More details can be found in Ref. [43]. In the middle loop, contact pressure is solve by Equation (9), and micro deformation on the seal lip is solved by Equations (14)–(17). Then, the follow convergence criterion equation is solved,

$$\frac{\left|\iint p(x,y)\,dxdy - \iint \left(p_f(x,y) + p_c(x,y)\right)dxdy\right|}{\iint p(x,y)\,dxdy} \le \varepsilon \tag{29}$$

where ε is the convergence tolerance. If the convergence criterion is met, solve the outermost loop, else, update the film thickness and return to the fluid pressure calculation. In the outermost loop, the continuous stroke of the seal is approximated as a discrete set of time. For each time step, the asperity contact pressure is solved. When the stroke, here assumed to be equal to the texture length L, is reached, the average asperity contact pressure is solved to predict the seal wear.

5. Procedure of the Simulation Method

The computational procedure is presented in Figure 6. The mixed lubricating model is firstly solved, then the wear model is solved based on the lubrication analysis. In the lubrication analysis, the fluid mechanics, asperity contact mechanics, and the micro deformation of the sealing lip are stronglyMaterials **2020**coupled, 13, 4458. In order to solve this coupling problem, an iterative method is adopted in10 of the28 numerical analysis.

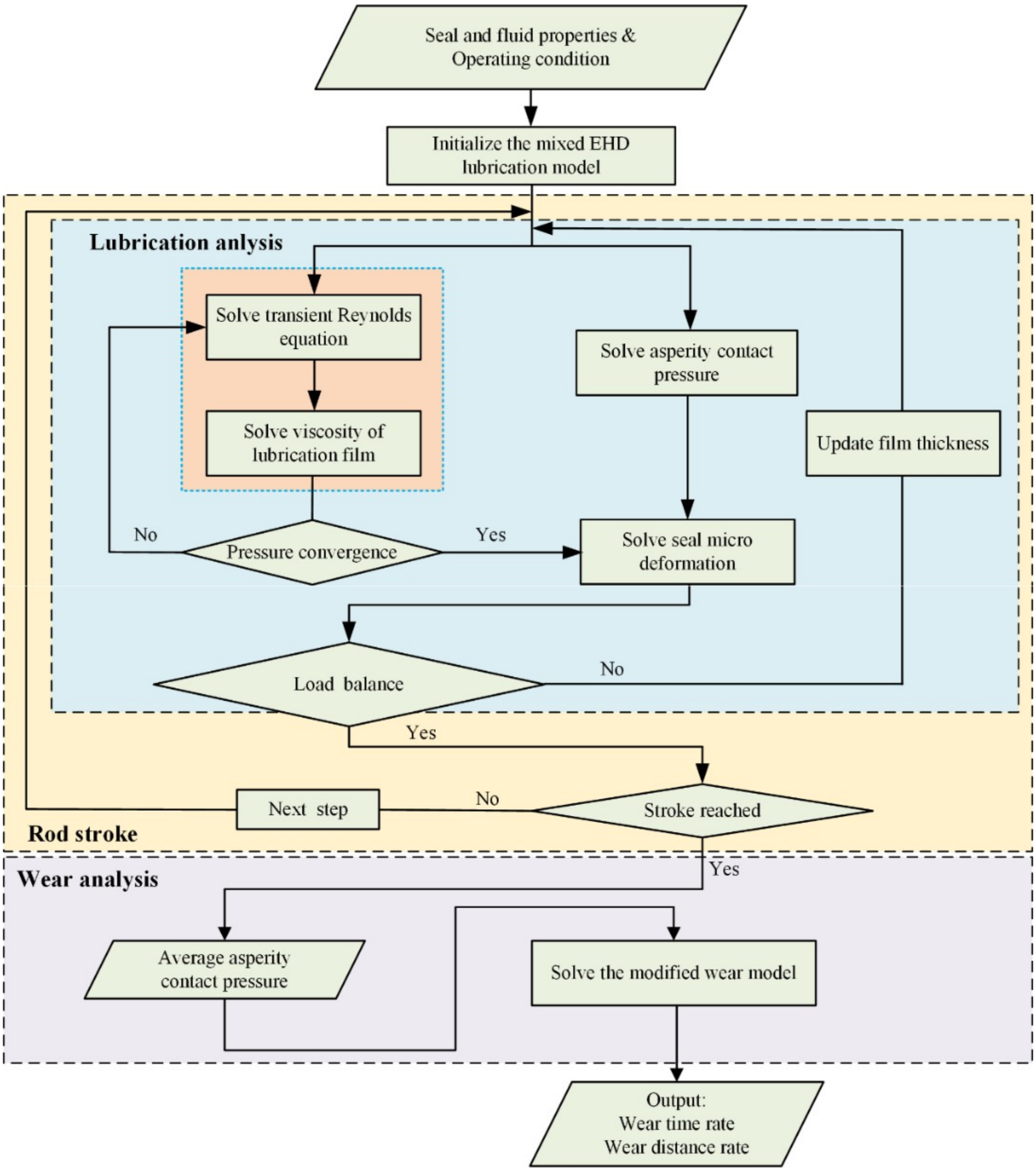

Figure 6. Scheme of computational procedure.

6. Results and Discussion

Wear of reciprocating seals with textured rod can be predicted by the proposed method. The main parameters are shown in Table 2, including seal face roughness, diameter of the rod, and so on. The sealed pressure is 5 MPa. By the FEA, the static contact pressure distributions are obtained, as shown in Figure 7. The maximum of the contact pressure is about 33.562 MPa and the contact width of the seal is about 0.19 mm. Table 3 shows the main geometrical parameters of the rod textures in the simulations.

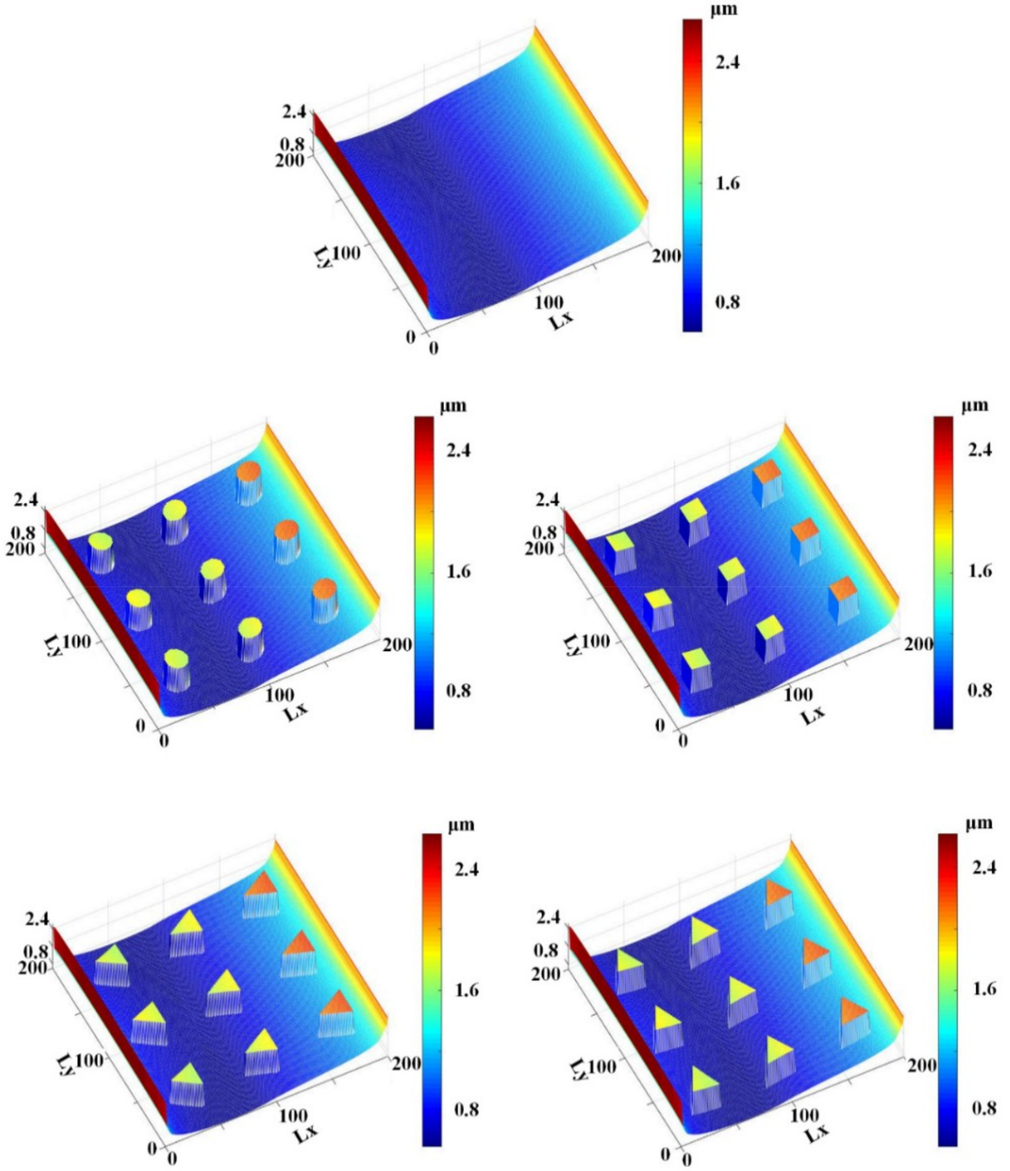

Figure1212.. Fililm **thickne**ss duringtheinstroke..

Figures1113and1214 show the asperitysimulationcontactresultspressureofthedistributionslubricatingonfilmtheonsealingthe sealingzonewithzone

withdifferenterenttextexturedrodsrod.As,showndurigintheFigureoutstroke13,theandasperityinstroke,contactrespectivelyressures.ofAstheshowntexturedin Figurerodare11,

durinbggerthethanoutstrokethoseofthethefilmsmooththicknessrodduringthe texturedtheoutstrzoneke, isexceptmuchingreaterthetexturedthanthatzonein. theAs mentionednon-textured

zone, of the shapes. It is reasonable shown in (3) and (7),

in the textured zone is thus very weak. According to the micro deformation analysis of the seal the film thickness in the textured zone is h_r larger than that in the non-textured zone. In this case,

surface, the pressure difference in the textured zone is undertaken by the fluid and asperity contact

the film thickness distribution is like the shapes of the rod's surface micro-cavity. Since the film

in the non-textured zone, the asperity contact pressure in the non-textured zone is thus bigger than

thickness in the textured zone is much bigger than that in the non-textured zone, less asperity contact

that of the smooth rod. A stronger wear will exist on the seal surface in the non-textured zone.

will exist in the textured zone, resulting in weaker seal wear.

Figure 14 shows the asperity contact pressure distributions for the smooth and textured rods Figure 12 shows the film thickness distributions during the instroke. As is the case during the

seal during the instroke. As is the case during the outstroke, the asperity contact pressures with the

outstroke, the film thickness in the textured zone is greater than that in the non-textured zone. Less

textured rods are bigger than those with the smooth rod. In the textured zone there is little existing

asperity contact exists in the textured zone, and the seal wear is weaker. Comparing the film thickness

asperity contact, resulting in a weaker seal wear. In the non-textured zone, since the asperity contact

during the outstroke and instroke, the film thickness during the outstroke is smaller than that during pressure is bigger than that of the smooth rod, a stronger seal wear will exist.

instroke, regardless of the smooth or textured rod. Hence, a stronger seal wear will occur during the outstroke.

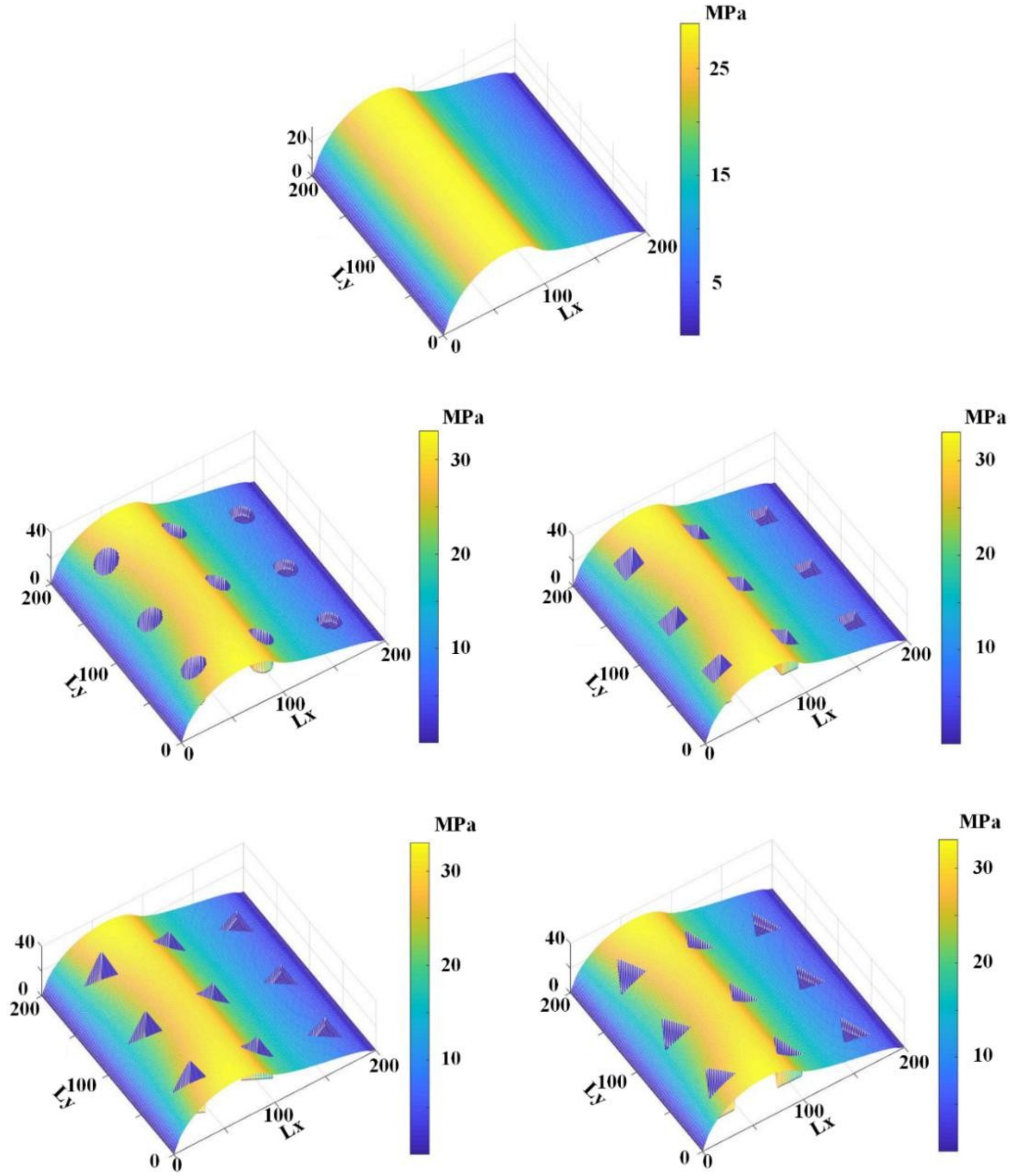

Figure 13. Asperity contact pressureduring theoutstroke.
13. the .

Figures 13 and 14 show the asperity contact pressure distributions on the sealing zone with di erent textured rods. As shown in Figure 13, the asperity contact pressures of the textured rod are bigger than those of the smooth rod during the outstroke, except in the textured zone. As mentioned above, the film in the textured zone is very thick, resulting in less asperity contact existing. Seal wear in the textured zone is thus very weak. According to the micro deformation analysis of the seal surface, the pressure di erence in the textured zone is undertaken by the fluid and asperity contact in the non-textured zone, the asperity contact pressure in the non-textured zone is thus bigger than that of the smooth rod. A stronger wear will exist on the seal surface in the non-textured zone.

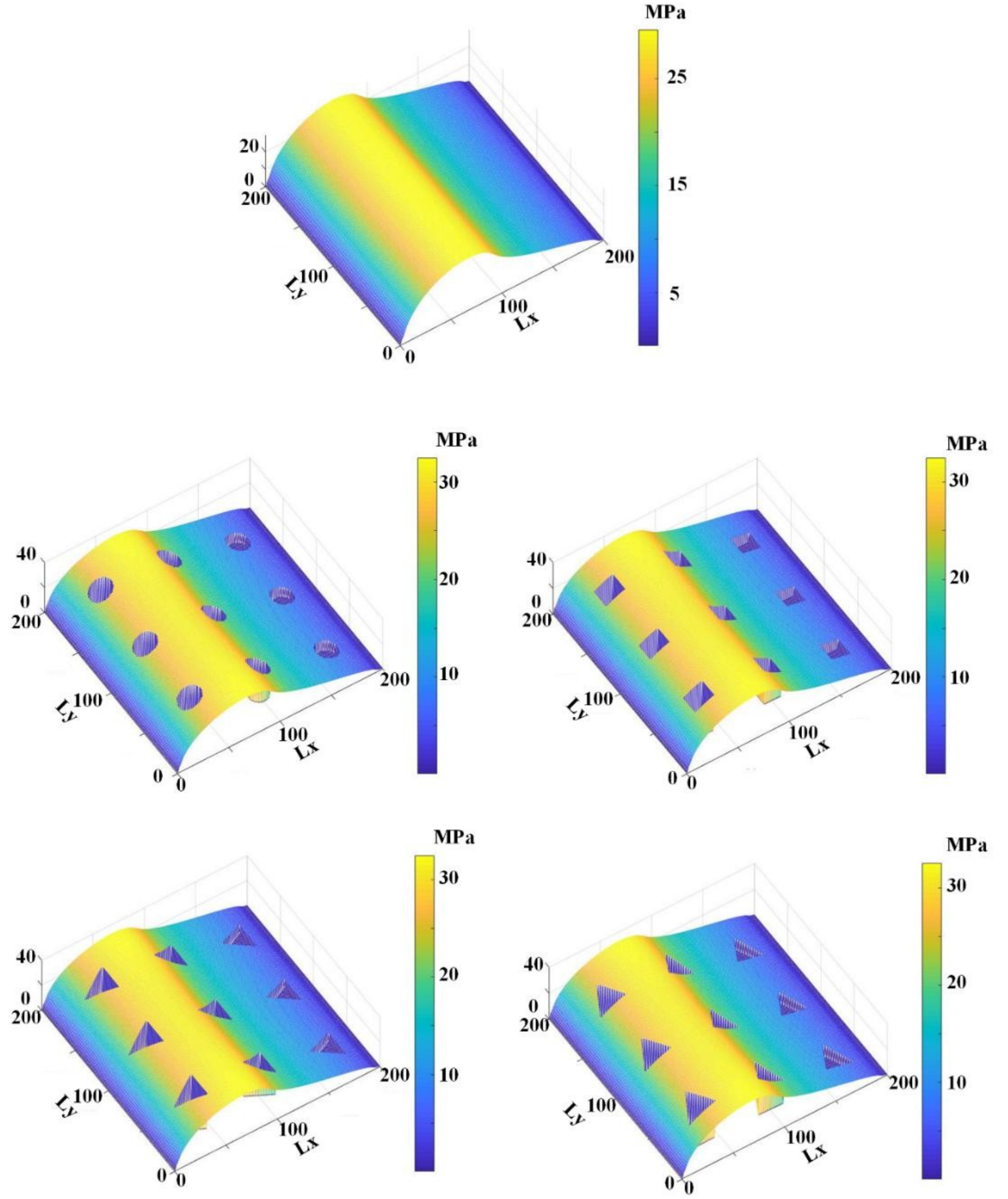

Figure 14. Asperity contact pressureduring theinstroke.
14. the .

Figure 14 shows the asperity contact pressure distributions for the smooth and textured rods Figures 15 and 16 show the simulation results of wear time rates and fluid flow rates, seal during the instroke. As is the case during the outstroke, the asperity contact pressures with the respectively. As shown in Figure 15, it can be noted that, during the outstroke, the textured rods will textured rods are bigger than those with the smooth rod. In the textured zone there is little existing significantly increase the seal wear compared with the smooth rod, but during the instroke the asperity contact, resulting in a weaker seal wear. In the non-textured zone, since the asperity contact increase is very small. The above-mentioned phenomena are in accordance with those in the analysis pressure is bigger than that of the smooth rod, a stronger seal wear will exist.
of the fluid pressure distribution. The average seal wear rate of the outstroke and instroke with the
Figures 15 and 16 show the simulation results of wear time rates and fluid flow rates, respectively. textured rod is a little bigger than that with smooth rod. Hence, it can be concluded that the effect of As shown in Figure 15, it can be noted that, during the outstroke, the textured rods will significantly the rod texture on the seal wear is negative. In addition, it can be noted that the effects of the textures increase the seal wear compared with the smooth rod, but during the instroke the increase is very small.
on the seal wear are almost identical.
The above-mentioned phenomena are in accordance with those in the analysis of the fluid pressure Figure 16 shows the fluid flow rates during the outstroke and instroke for different kinds of distribution. The average seal wear rate of the outstroke and instroke with the textured rod is a little textures. Note that the flow rate of the textured rod is a little bigger than that of the smooth rod, bigger than that with smooth rod. Hence, it can be concluded that the e ect of the rod texture on the during both the outstroke and instroke. It should be emphasized that, since the rod speed is slow, the
fluid is carried out of the cylinder during the instroke. Therefore, the seal will leak during the instroke. In this case, the textured rod can reduce the seal leakage during both the outstroke and

seal wear is negative. instroke, as shown in in In addition, it can be noted that the e ects of the textures on the seal wear are Figure 16. Moreover, the effects of the textured rods on the seal leakage are almost identical. . of

basically the same.

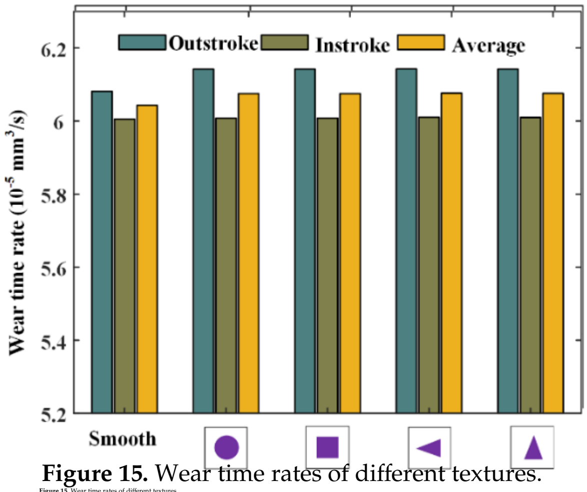

Figure 15. Wear time rates of different textures.

Figure 15. Wear time rates of different textures.

Figure 15. Wear time rates of di erent textures.

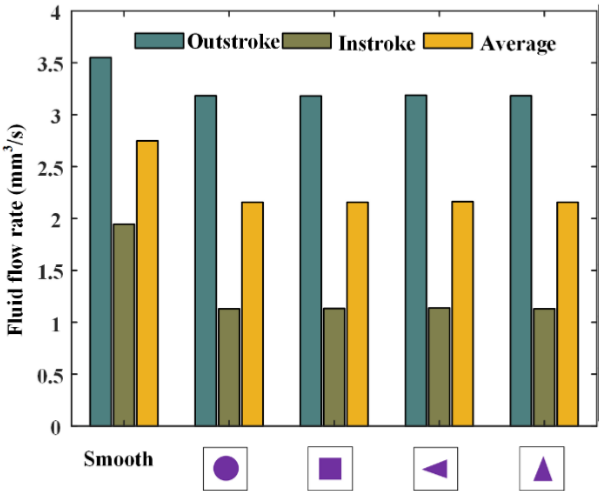

Figure 16. Fluid flow rates of different textures.

Figure 16. Fluid flow rates of textures.

Figure 16. Fluid flow rates ofdifferent textures.

In the numerical calculation of the seal wear, simulation space on the sealing zone should be Figure 16 shows the fluid fl w rates during thesi outstroke nd i stroke for di er nt kin s of meshed. When the mesh is 200 × 200, 180 × 180, and 150 × 150, the simulation results of the circle textures.. Note that the flowis rate of× the textured× rod is little×bigger than that of the smoothofrod, duci ing bo h the outstroke instroke. It should be emphasized that, since the rod speed slow, the fluid is calculation mesh. When the mesh changes from 200 × 200 to 150 × 150, the value of the wear rate carried out of the. cylinder during the instroke. Therefore,× thetoseal will× leak during theofinstroke. In this case, the textured3. rod can reduce the seal leakage during4. both the outin .and instroke as shown toin increase the element density of the mesh in the numerical simulation to improve the accuracy of the Figure 16. Moreover, the ectsof of the texturedin rods on the seal leakageto are basically the same. of

In the numerical calculation of the seal wear, is simulation space. on the sealing zone should be meshed. When the mesh is 200 200, 180 180, and 150 150, the simulation results of the circle texture are shown in Figure 17. It can be seen that the simulation wear rate is a ected by the calculation mesh. When the mesh changes from 200 200 to 150 150, the value of the wear rate increases by 3.9% during outstroke, and increases by 4.8% during instroke. To this end, we need to increase the element density of the mesh in the numerical simulation to improve the accuracy of the wear calculation, although the simulation time is thus increased.

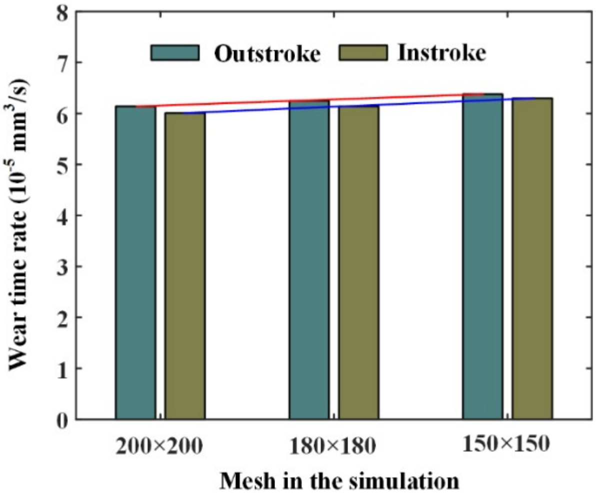

Figure 17. Wear rates under different simulation meshes.

Figure 17. Wear rates under different simulation meshes.

6.3. Effects of Rod Speed

6.3. Effects of Rod Speed

Seal wear with different textured rods under different rod speeds is also simulated, as shown in Figures 18 and 19. In Figure 18, the asperity contact load ratio increases with rod speed increasing during the outstroke, regardless of the texture shapes. However, during the instroke the contact load ratio increases. It indicates that, during the instroke the fluid pressure increases with rod speed, and the seal lip is thus pushed higher, moving away from the rod surface. However, during the outstroke the fluid pressure is weakened by rod speed increasing, resulting in the rod's surface being closer to the lip seal. In addition, the asperity contact load ratios of different textures are similar to each other, which is in accordance with the analysis of Figures 13 and 14. Hence, the seal wear of different textured rods is similar to each other too. Through Figure 18, it can be seen that the operating conditions would significantly affect the lubrication of the rod seal, seal wear is thus changed with conditions. Asperity contact load ratios during the outstroke are a little bigger than those during the instroke. Hence, the wear of the reciprocating seal during the outstroke will be greater than that during instroke, regardless of the rod speed.

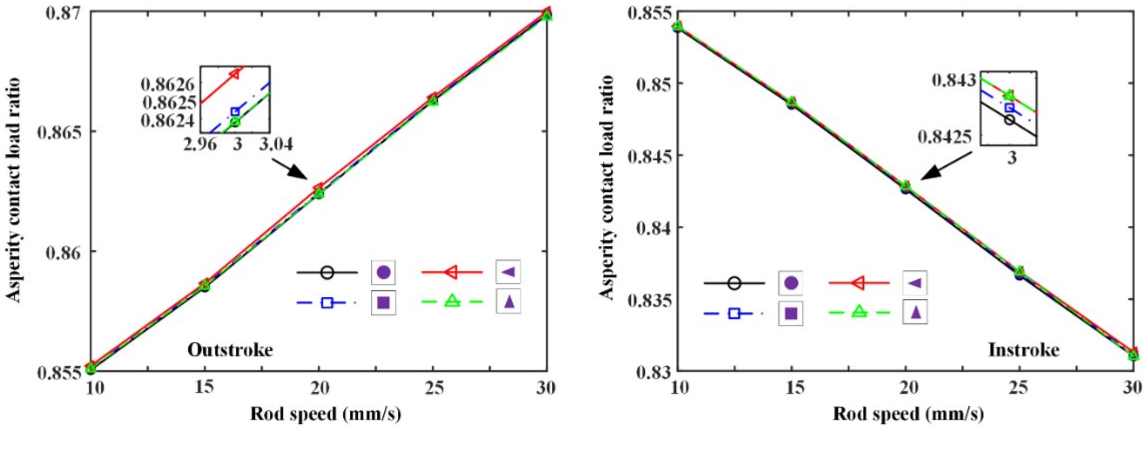

(**a**) (**b**)

Figure 18. The relationship between the rod speeds and asperity contact load ratios, (**a**) outstroke, (**b**) instroke.

The average wear rate is defined as the mean value of the outstroke and instroke, and the simulation results of different textures are shown in Figure 19. Note that when the rod's speed is increasing from 10 mm/s to 30 mm/s, the average wear distance rates decrease from about 3.08×10^{-6} mm^3/mm to about 3.02×10^{-6} mm^3/mm. It is because of this, the increase in the seal wear during the outstroke is smaller than the seal wear decrease during the instroke. In addition, with the rod's speed increasing, average wear time rates increase from about 3.1×10^{-5} mm^3/s to about 9.1×10^{-5} mm^3/s. It can be concluded that the service lifetime of the seal will be reduced with the increased rod speed.

Therefore, when analyzing the seal wear with the textured rod, the operating condition of the rod's speed should be considered.

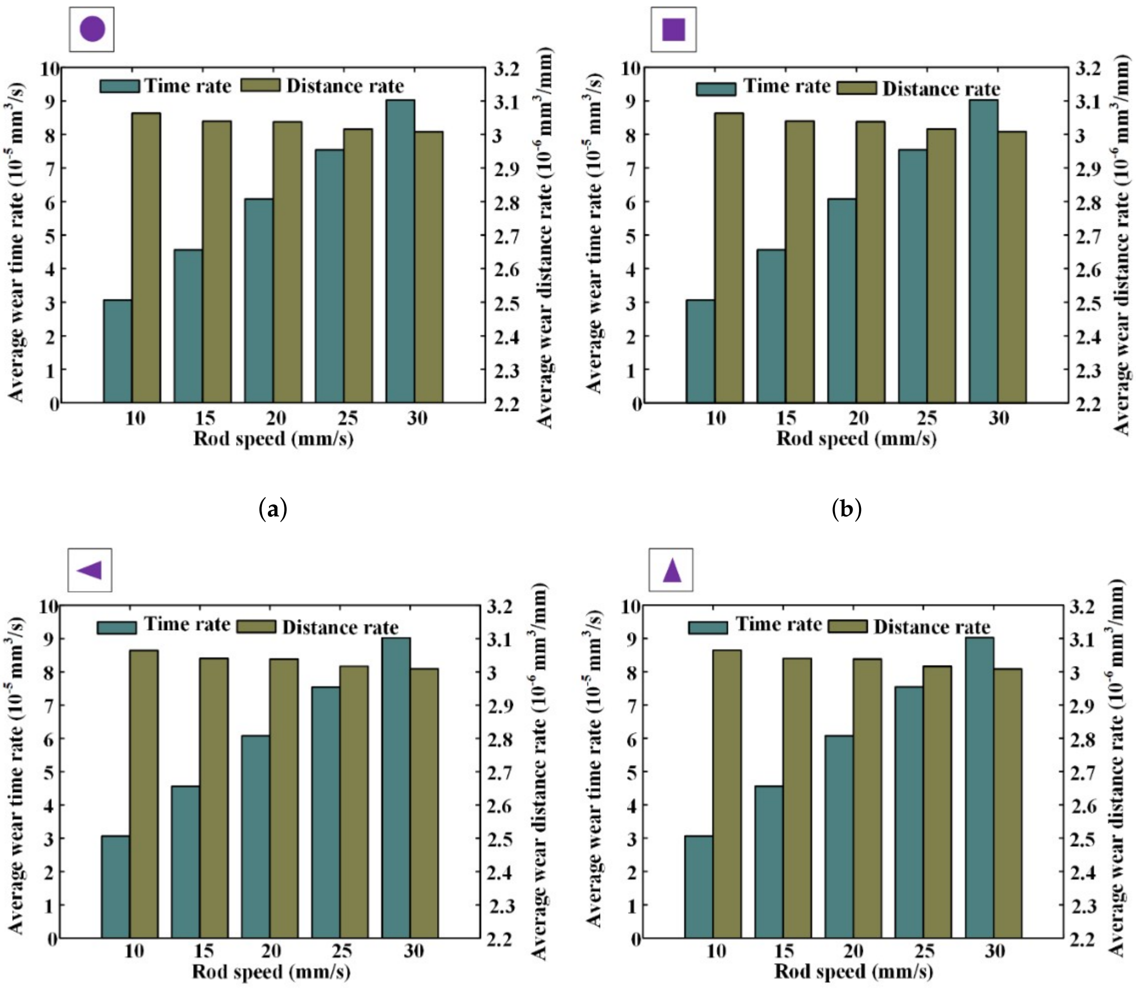

(a) (b)

(c) (d)

Figure 19. The wear rates under di erent rod speeds, (**a**) circle, (**b**) square, (**c**) triangle (Axial symmetry), (**d**) triangle (Circumferential symmetry).

Figure 19. The wear rates under different rod speeds, (a) circle, (b) square, (c) triangle (Axial symmetry), (d) triangle (Circumferential symmetry).

Figures 20 and 21 show the seal wear rates and fluid flow rates with di erent texture area ratios, respectively. Corresponding simulation parameters are: rod speed 20 mm/s, texture depth 1.3 m, shape feature parameter one, and texture area ratio 0.06–0.1.

In Figure 20, it can be noted that, with texture area ratio increasing, wear time rates increase during outstroke, regardless of the texture shapes. During the instroke, the wear time rates increase too. It is because of this that with the texture area ratio increasing, the pressure di erence in the textured zone increases, resulting in a bigger load on the non-textured zone. The sealing lip is thus closer to the rod's surface and the lubricating film becomes thinner. In this case, the sear wear in the non-textured zone becomes worse. If the increase in the seal wear in the non-textured zone is bigger than the decrease in the textured zone, the seal wear will increase, as shown in Figure 20.

As shown in Figure 21, with the texture area ratio increasing, the fluid flow rates are decreased during both the outstroke and instroke. It is because that, with the increase of the texture area ratio, the pressure di erence in the textured zone increases.The seal lip is thus pushed closer to the rod's surface and the film thickness in the sealing zone becomes thinner. Hence, the fluid flow rate of the seal is decreased with the increasing texture area ratio.

Figures 22 and 23 show the seal wear rates and fluid flow rates with di erent texture depths, respectively. The corresponding simulation parameters are: rod speed 20 mm/s, texture area ratio 0.08, shape feature parameter one, and texture depth 1–3 m.

As shown in Figure 22, it can be noted that, with texture depth increasing the wear of the seal decreases during the outstroke, regardless of the texture shapes. However, during the instroke the seal wear increases when the texture depth increases. This means that, with texture depth increasing, the fluid pressure increases during the outstroke, while it decreases during the instroke. As shown in Figure 23, it can be noted that the fluid flow rates decrease with the increasing texture depth during the outstroke, regardless of the texture shapes. This is because that, although the fluid pressure in the textured zone increases during the outstroke, when the texture depth increases, the asperity contact pressure in the textured zone decreases, the whole pressure in the textured decreases. In this case, the asperity contact pressure in the non-textured zone increases and the lubricating film on the sealing zone of the textured rod is decreased. Hence, the fluid flow rate decreases. During the instroke, the fluid flow rates decrease too. It is because of this that during the instroke the fluid pressure and the asperity contact pressure in the textured zone decrease with increasing texture depth. So, the asperity contact pressure in the non-textured zone increases. In this case, the lubricating film becomes thinner and the fluid flow rate decreases.

Through the analysis of Figures 20 and 21, increasing the texture depth is a possible way to increase the seal performance, since it can reduce the leakage of the seal, while it may not increase the wear rate.

Wear time rates and fluid flow rates with di erent texture feature parameters were also numerically investigated, the simulation results are shown in Figures 24 and 25. Corresponding simulation parameters are: rod speed 20 mm/s, texture area ratio 0.08, texture depth 1.3 m, and shape feature parameter 0.8–1.2.

Figure 24 shows the wear time rates with di erent shape feature parameters, during the outstroke and instroke. Note that, with the feature parameter increasing, the wear time rates are nearly unchanged, regardless of the textures shapes. This is because with the feature parameter increasing, the pressure di erence of the textured zone in the x-axis direction increases, and in the y-axis direction decreases, the pressure di erence in the whole textured zone is thus unchanged. Hence, the load of the asperity contact on the sealing zone has no change, resulting in an unchanged of the seal wear rate.

The fluid flow rates with di erent shape feature parameters of the textures are shown in Figure 25. It can be seen that the fluid flow rates have no change with the increasing feature parameter. As mentioned above, with the shape feature parameter increasing, the pressure di erence in the whole textured zone is unchanged, resulting in an unchanged load in the non-textured zone. So, the film thickness on the sealing zone is unchanged, and the fluid flow rate has no change.

7. Conclusions

In this paper, a numerical model is presented to investigate the e ects of the textured rods on the wear of the reciprocating seal. This model is focused on the seal wear under mixed lubrication conditions by combining the EHD lubrication model and the Archard wear model. An iterative algorithm is used to solve the lubrication model, since the fluid pressure, asperity contact pressure and micro-deformation of the seal lip are strongly coupled. A comparison of the average asperity contact pressure on the simulation space between the present model and Huang's model is carried out to validate the model in the present research. The e ects of the mesh in the numerical simulation are analyzed. Seal wear under di erent rod speeds are simulated and analyzed. Importantly, the e ects of the texture on the seal wear are parametrically studied.

The textures on rod surface have a significant influence on the fluid pressure, film thickness and asperity contact pressure distributions. Since the wear of the seal lip greatly depends on the asperity contact of the seal with the rod surface, the texture e ects cannot be neglected. Compared with the smooth rod, the textured rod will increase the seal wear, but reduce the seal leakage. Under the same sealed pressure, the seal during the outstroke seems to have a higher risk of wear than during the instroke, and should be receive more attention in the seal design. With the texture area ratio increasing, the seal wear increases and the leakage decreases, regardless of the texture shapes. When the texture depth increases, the seal leakage decreases, the seal wear decreases during the outstroke and increases during the instroke. The shape feature parameter has no e ect on the wear and the leakage of the reciprocating rod seal. In addition, rod speed is one of the most important factors for analyzing the seal wear and needs to be considered in the analysis of the seal wear with textured rods. The simulation results are sensitized to the mesh in that it needs to increase elements density of the mesh to improve the accuracy of the wear calculation.

The presented research provides a foundation for engineers to investigate the seal wear of the reciprocating seal with textured rods. The e ects of start/stop of the rod are ignored in the present model, but the start/stop of the rod exacerbates the seal wear since the seal surface traps in the micro-cavity on rod surface when the rod is stationary. Therefore, the e ects of start/stop of the rod and experimental verifications should be focused on in future research.

Author Contributions: The manuscript was written with the contribution of all authors. H.R. carried out the simulation and write the original draft, D.L. proposed the idea and reviewed the manuscript, S.W. analyzed the data and reviewed the manuscript. All authors have read and agreed to the published version of the manuscript.

Funding: This study was supported by Natural Science Foundation of China: 51620105010, and Natural Science Foundation of Beijing Municipality: L171003.

Acknowledgments: Thanks are due to Chao Zhang for valuable discussion.

Conflicts of Interest: The authors declare no conflict of interest.

List of Symbols

a length of micro-cavity in axial direction	b length of micro-cavity in circumferential direction
C_{10}, C_{01}, d Mooney–Rivlin coe cients	D_{rod} rod diameter
E equivalent Young's modulus	E_{seal} Young's modulus of the seal
F cavitation factor	F_{sum} sum of the pressure di erences
h film thickness	h_0 initial film thickness
h_p depth of the micro-cavity	h_r rod surface height
h_T average truncated film thickness	h_W wear depth
Dh micro deformation of the sealing lip surface	H hardness
I_1, I_2 deviatoric strain invariants	J parameter relating to the elastic deformation gradient
k wear modulus	K wear coe cient
L side length of texture	L_x length of the simulation space in axial direction

References

1. Liao, B.; Sun, B.; Li, Y.; Yan, M.; Ren, Y.; Feng, Q.; Yang, D.; Zhou, K. Sealing reliability modeling of aviation seal based on interval uncertainty method and multidimensional response surface. Chin. J. Aeronaut. **2019**, 32, 2188–2198. [CrossRef]
2. Zhang, C.; Chen, R.; Bai, G.; Wang, S.; Tomovic, M.M. Reliability estimation of rotary lip seal in aircraft utility system based on time-varying dependence degradation model and its experimental validation. Chin. J. Aeronaut. **2019**. [CrossRef]
3. Wang, J.; Li, Y.; Lian, Z. Numerical Investigations on the Sealing Performance of a Reciprocating Seal Based on the Inverse Lubrication Method. J. Tribol. **2019**, 141, 112201. [CrossRef]
4. Peng, C.; Guo, S.; Ouyang, X.; Zhou, Q.; Yang, H. An eccentric 3-D fluid-structure interaction model for investigating the effects of rod parallel offset on reciprocating-seal performance. Tribol. Int. **2018**, 128, 279–290. [CrossRef]
5. Wang, B.; Peng, X.-D.; Meng, X.-K. A thermo-elastohydrodynamic lubrication model for hydraulic rod O-ring seals under mixed lubrication conditions. Tribol. Int. **2019**, 129, 442–458. [CrossRef]
6. Xiang, C.; Guo, F.; Jia, X.; Wang, Y.; Huang, X. Thermo-elastohydrodynamic mixed-lubrication model for reciprocating rod seals. Tribol. Int. **2019**, 140, 105894. [CrossRef]
7. Peng, C.; Guo, S.; Ouyang, X.; Zhou, Q.; Yang, H. Mixed Lubrication Modeling of Reciprocating Seals Based on a Developed Multiple-Grid Method. Tribol. Trans. **2018**, 61, 1151–1161. [CrossRef]
8. Huang, Y.; Salant, R.F. Numerical analysis of a hydraulic rod seal: Flooded vs. starved conditions. Tribol. Int. **2015**, 92, 577–584. [CrossRef]
9. Bhaumik, S.; Kumaraswamy, A.; Guruprasad, S.; Bhandari, P. Investigation of friction in rectangular Nitrile-Butadiene Rubber (NBR) hydraulic rod seals for defence applications. J. Mech. Sci. Technol. **2015**, 29, 4793–4799. [CrossRef]
10. Zhang, H.; Hua, M.; Dong, G.-N.; Zhang, D.; Chin, K. A mixed lubrication model for studying tribological behaviors of surface texturing. Tribol. Int. **2016**, 93, 583–592. [CrossRef]
11. Gu, C.; Meng, X.; Xie, Y.; Fan, J. A thermal mixed lubrication model to study the textured ring/liner conjunction. Tribol. Int. **2016**, 101, 178–193. [CrossRef]
12. Gu, C.; Meng, X.; Xie, Y.; Yang, Y. E ects of surface texturing on ring/liner friction under starved lubrication. Tribol. Int. **2016**, 94, 591–605. [CrossRef]
13. Huang, Y.; Salant, R.F. Simulation of the E ects of a Plunge Ground Rod on Hydraulic Rod Seal Behavior. Tribol. Trans. **2013**, 56, 986–996. [CrossRef]
14. Huang, Y.; Salant, R.F. Simulation of a hydraulic rod seal with a textured rod and starvation. Tribol. Int. **2016**, 95, 306–315. [CrossRef]

15. El Gadari, M.; Hajjam, M. E ect of the Grooved Rod on the Friction Force of U-Cup Hydraulic Rod Seal with Rough Lip. Tribol. Trans. **2018**, 61, 661–670. [CrossRef]
16. Guo, F.; Jia, X.; Gao, Z.; Wang, Y. The e ect of texture on the shaft surface on the sealing performance of radial lip seals. Sci. China Ser. G Phys. Mech. Astron. **2014**, 57, 1343–1351. [CrossRef]
17. Guo, F.; Jia, X.; Wang, L.; Wang, Y. The e ect of axial position of contact zone on the performance of radial lip seals with a texturing shaft surface. Tribol. Int. **2016**, 97, 499–508. [CrossRef]
18. Zhao, X.; He, X.; Wang, L.; Chen, P. Research on pressure compensation and friction characteristics of piston rod seals with di erent degrees of wear. Tribol. Int. **2020**, 142, 105999. [CrossRef]
19. Guo, F.; Jia, X.; Longke, W.; Salant, R.F.; Wang, Y. The E ect of Wear on the Performance of a Rotary Lip Seal. J. Tribol. **2014**, 136, 041703. [CrossRef]
20. Lee, S.; Yoo, S.; Kim, D.-E.; Kang, B.; Kim, H. Accelerated wear test of FKM elastomer for life prediction of seals. Polym. Test. **2012**, 31, 993–1000. [CrossRef]
21. Mofidi, M.; Prakash, B. The Influence of Lubrication on Two-body Abrasive Wear of Sealing Elastomers Under Reciprocating Sliding Conditions. J. Elastomers Plast. **2010**, 43, 19–31. [CrossRef]
22. Farfán-Cabrera, L.I.; Gallardo-Hernández, E.A.; De La Rosa, C.S.; Vite-Torres, M. Micro-scale abrasive wear of some sealing elastomers. Wear **2017**, 1347–1355. [CrossRef]
23. Frölich, D.; Magyar, B.; Sauer, B. A comprehensive model of wear, friction and contact temperature in radial shaft seals. Wear **2014**, 311, 71–80. [CrossRef]
24. Belhocine, A.-; Ghazaly, N.M. E ects of material properties on generation of brake squeal noise using finite element method. Lat. Am. J. Solids Struct. **2015**, 12, 1432–1447. [CrossRef]
25. Sui, H.; Pohl, H.; Schomburg, U.; Upper, G.; Heine, S. Wear and friction of PTFE seals. Wear **1999**, 224, 175–182. [CrossRef]
26. Békési, N.; Varadi, K. Wear simulation of a reciprocating seal by global remeshing. Period. Polytech. Mech. Eng. **2010**, 54, 71. [CrossRef]
27. Békési, N.; Varadi, K.; Felh˝os, D. Wear Simulation of a Reciprocating Seal. J. Tribol. **2011**, 133, 031601. [CrossRef]
28. Xin, L.; Gaoliang, P.; Zhe, L. Prediction of seal wear with thermal–structural coupled finite element method. Finite Elements Anal. Des. **2014**, 83, 10–21. [CrossRef]
29. Xin, L.; Peng, G.; Qiang, W.; Yuhui, L. A Numerical Analysis Method of Hydraulic Seals for Downhole Equipments. Adv. Mech. Eng. **2013**, 5, 151794. [CrossRef]
30. Angerhausen, J.; Woyciniuk, M.; Murrenho , H.; Schmitz, K. Simulation and experimental validation of translational hydraulic seal wear. Tribol. Int. **2019**, 134, 296–307. [CrossRef]
31. Ran, H.; Wang, S.; Liu, D. A multiscale wear model for reciprocating rod stepseal under mixed lubricating conditions based on linear elasticity. Proc. Inst. Mech. Eng. Part J J. Eng. Tribol. **2020**, 1–20. [CrossRef]
32. Liu, D.; Wang, S.; Zhang, C. A multiscale wear simulation method for rotary lip seal under mixed lubricating conditions. Tribol. Int. **2018**, 121, 190–203. [CrossRef]
33. Xiong, D.; Qin, Y.; Li, J.; Wan, Y.; Tyagi, R. Tribological properties of PTFE/laser surface textured stainless steel under starved oil lubrication. Tribol. Int. **2015**, 82, 305–310. [CrossRef]
34. Shi, Y.; Feng, X.; Wang, H.; Lü, X. Tribological properties of PTFE composites filled with surface-treated carbon fiber. J. Mater. Sci. **2007**, 42, 8465–8469. [CrossRef]
35. Liu, D.; Wang, S.; Zhang, C.; Tomovic, M.M. Numerical study of the e ects of textured shaft on the wear of rotary lip seals. Tribol. Int. **2019**, 138, 215–238. [CrossRef]
36. Payvar, P.; Salant, R.F. A Computational Method for Cavitation in a Wavy Mechanical Seal. J. Tribol. **1992**, 114, 199–204. [CrossRef]
37. Patir, N.; Cheng, H.S. Application of Average Flow Model to Lubrication Between Rough Sliding Surfaces. J. Lubr. Technol. **1979**, 101, 220–229. [CrossRef]
38. Greenwood, J.A.; Tripp, J.H. The Contact of Two Nominally Flat Rough Surfaces. Proc. Inst. Mech. Eng. **1970**, 185, 625–633. [CrossRef]
39. Guo, F.; Jia, X.; Suo, S.; Salant, R.F.; Wang, Y. A mixed lubrication model of a rotary lip seal using flow factors. Tribol. Int. **2013**, 57, 195–201. [CrossRef]
40. Liu, W.; He, G.; Weikai, L.; Guoqiang, H. Storage life of silicone rubber sealing ring used in solid rocket motor. Chin. J. Aeronaut. **2014**, 27, 1469–1476. [CrossRef]